Flying plasmonic lens in the near field for high-speed nanolithography

WERAYUT SRITURAVANICH†, LIANG PAN†, YUAN WANG†, CHENG SUN, DAVID B. BOGY AND XIANG ZHANG*

Department of Mechanical Engineering, University of California, Berkeley, California 94720-1740, USA
†These authors contributed equally to this work.
***e-mail: xiang@berkeley.edu**

Published online: 12 October 2008; corrected online: 4 November 2008; doi:10.1038/nnano.2008.303

The commercialization of nanoscale devices requires the development of high-throughput nanofabrication technologies that allow frequent design changes[1,2]. Maskless nanolithography[3–13], including electron-beam and scanning-probe lithography, offers the desired flexibility but is limited by low throughput. Here, we report a new low-cost, high-throughput approach to maskless nanolithography that uses an array of plasmonic lenses that 'flies' above the surface to be patterned, concentrating short-wavelength surface plasmons into sub-100 nm spots. However, these nanoscale spots are only formed in the near field, which makes it very difficult to scan the array above the surface at high speed. To overcome this problem we have designed a self-spacing air bearing that can fly the array just 20 nm above a disk that is spinning at speeds of between 4 and 12 m s^{-1}, and have experimentally demonstrated patterning with a linewidth of 80 nm. This low-cost nanofabrication scheme has the potential to achieve throughputs that are two to five orders of magnitude higher than other maskless techniques.

Optical lithography[1,2] has been the workhorse for the semiconductor industry in recent decades, and although the resolution of this technique has continued to improve, there have also been substantial increases in costs. The price of a typical single lithography tool is close to $20 million. The fabrication of high-quality lithography masks has also become time consuming and expensive, which hinders device prototyping, where frequent design changes are often needed. Maskless nanolithography, including electron-beam, focused ion-beam[3] and scanning-probe lithography[4–6] (SPL), offers a path to overcome these obstacles by reducing mask costs and shortening the cycle time for nanoscale device validation[7]. However, the low throughput of these maskless methods due to the serial and slow scanning process that is involved remains a bottleneck. Although multi-axial electron-beam lithography[8–10] has been proposed to increase throughput by using multiple electron beams in a parallel manner, there are difficulties in simultaneously regulating the multiple beam sizes and beam positions because of the thermal drift and electrical charge Coulomb interactions, which result in significant lens aberration. This has made its future uncertain. Zone-plate-array lithography[11] (ZPAL), uses a large array of diffractive optical elements or spatial light modulators to improve the throughput, but the ultimate resolution is still restricted to the diffraction limit. SPL, a tip-based, low-cost

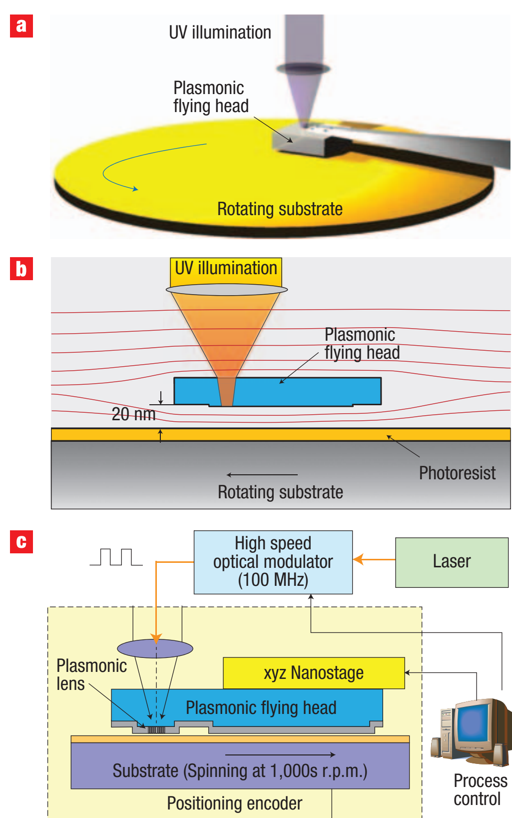

Figure 1 High-throughput maskless nanolithography using plasmonic lens arrays. a, Schematic showing the lens array focusing ultraviolet (365 nm) laser pulses onto the rotating substrate to concentrate surface plasmons into sub-100 nm spots. However, sub-100 nm spots are only produced in the near field of the lens, so a process control system is needed to maintain the gap between the lens and the substrate at 20 nm. **b**, Cross-section schematic of the plasmonic head flying 20 nm above the rotating substrate which is covered with photoresist. **c**, Schematic of process control system. The laser pulses are controlled by a high-speed optical modulator according to the signals from a pattern generator. The writing position is referred to the angular position of the disk from the spindle encoder and the position of a nano-stage along the radial direction.

© 2008 Macmillan Publishers Limited. All rights reserved.

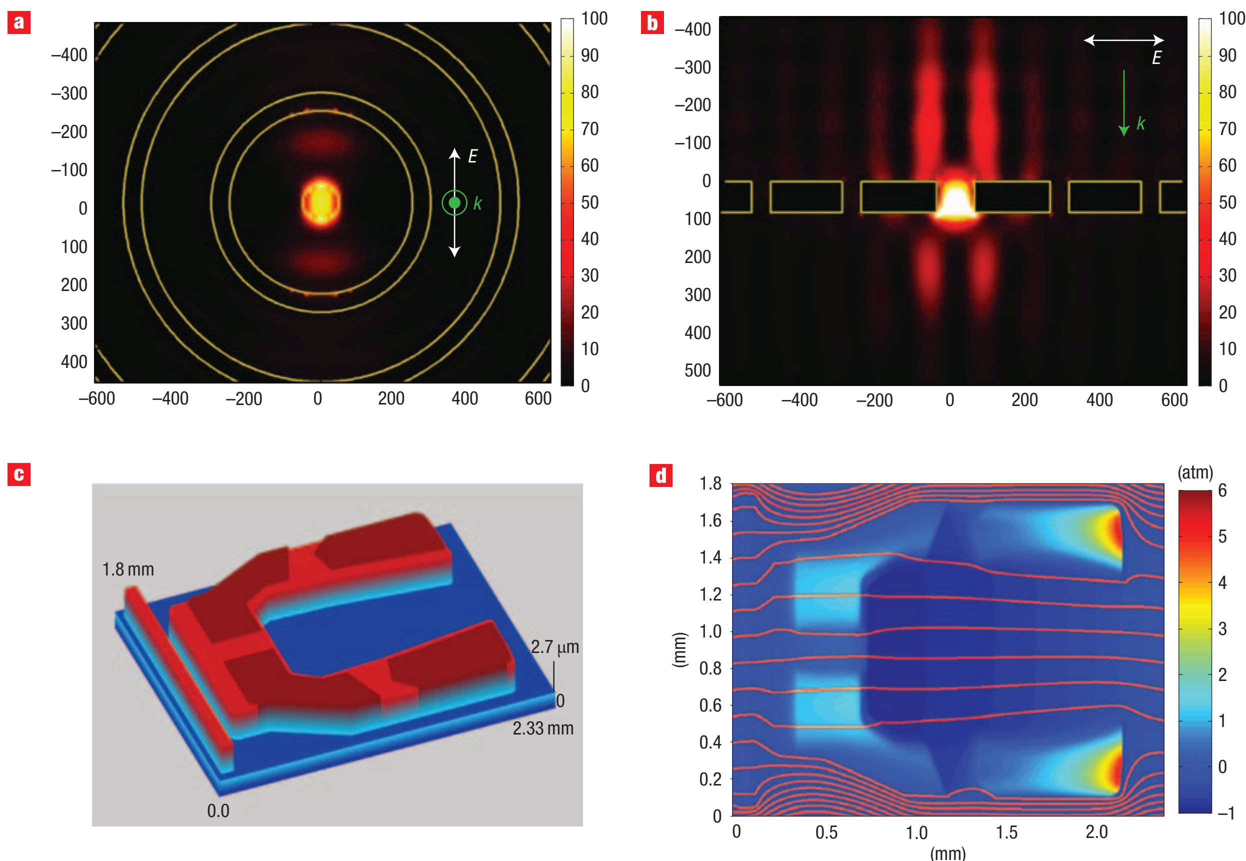

Figure 2 Designs and simulations for the plasmonic lens and an air-bearing surface (ABS). **a**, For a plasmonic lens composed of a nano-aperture surrounded by 15 through-rings on an aluminium film, calculated intensity 20 nm away from the lens under the linearly polarized light illumination at a wavelength of 365 nm. A tightly focused 80-nm spot can be obtained in the near field. The aperture diameter, ring periodicity, ring width and aluminium layer thickness are 100, 250, 50 and 80 nm, respectively. **b**, Cross-sectional view of the plasmonic lens and the intensity enhanced ~100 times at the focal point compared to that of the incident light. **c**, Oblique view of the ABS. The topography is scaled up by a factor of 200 for better illustration. The ABS generates an aerodynamic lift force and it is balanced with the force supplied by suspension to precisely retain a nanoscale gap between the plasmonic lens arrays and the rotating substrate. **d**, Calculated normal air pressure (coloured) and air-mass flow lines (from left to right) under the ABS with a scanning speed of 10 m s^{-1}. The pressure is normalized to ambient air pressure. The mass flow lines density is proportional to the mass flow. At the lowest point, the air pressure is maximized but the mass flow is minimized, which favours both air-bearing stiffness and contamination tolerance.

alternative operating in an ambient environment, has made a noticeable throughput improvement, as shown in a recent demonstration using 55,000 probes scanning at a speed of 60 µm s^{-1} (ref. 12). However, its throughput is still two to three orders of magnitude lower than that required by practical nanofabrication applications[13]. This is because SPL technology relies on a slow scan of the tips at a distance of 10–100 nm from the surface, owing to the limited feedback bandwidth available to control the tip–sample distance at higher speeds. We report here a novel high-throughput form of plasmonic nanolithography to circumvent the critical parallelization and slow scanning challenges. This can potentially increase throughput by two to five orders of magnitude compared to that achieved by parallel SPL and commercial electron-beam lithography.

When light strikes a metal surface it can excite collective oscillations of the electrons at the surface that are known as surface plasmons[14–16]. These oscillations can have wavelengths that are much shorter than the wavelength of the light that excited them, which means that surface plasmons could have applications for imaging[17] and lithography[18–20] with resolution beyond the diffraction limit. A plasmonic lens made of a concentric ring grating has been used to focus the light to a sub-100 nm spot at the near field with local intensity >100 times higher than the incident light[21] (see Supplementary Information). These earlier results clearly suggest the potential of using a plasmonic lens for nanolithography. However, owing to the exponential decay of the evanescent field, the tightly focused spot only exists at the near field of the plasmonic lens, normally closer than 100 nm. Thus, high-throughput nanopatterning requires a new mechanism to ensure precise control of the nanoscale gap between the plasmonic lens and substrate during high-speed writing.

We report here the first high-speed flying plasmonic lens arrays using an air bearing (Fig. 1). To achieve high-speed scanning while maintaining the nanoscale gap, we designed a novel air-bearing slider to fly the plasmonic lens arrays at a height of 20 nm above the substrate at speeds of between 4 and 12 m s^{-1}. The rotation of the substrate creates an air flow along the bottom surface of the plasmonic flying head, known as the air bearing surface (ABS). The ABS generates an aerodynamic lift force and it is balanced with the force supplied by the suspension arm to precisely regulate a nanoscale gap between the plasmonic lens

© 2008 Macmillan Publishers Limited. All rights reserved.

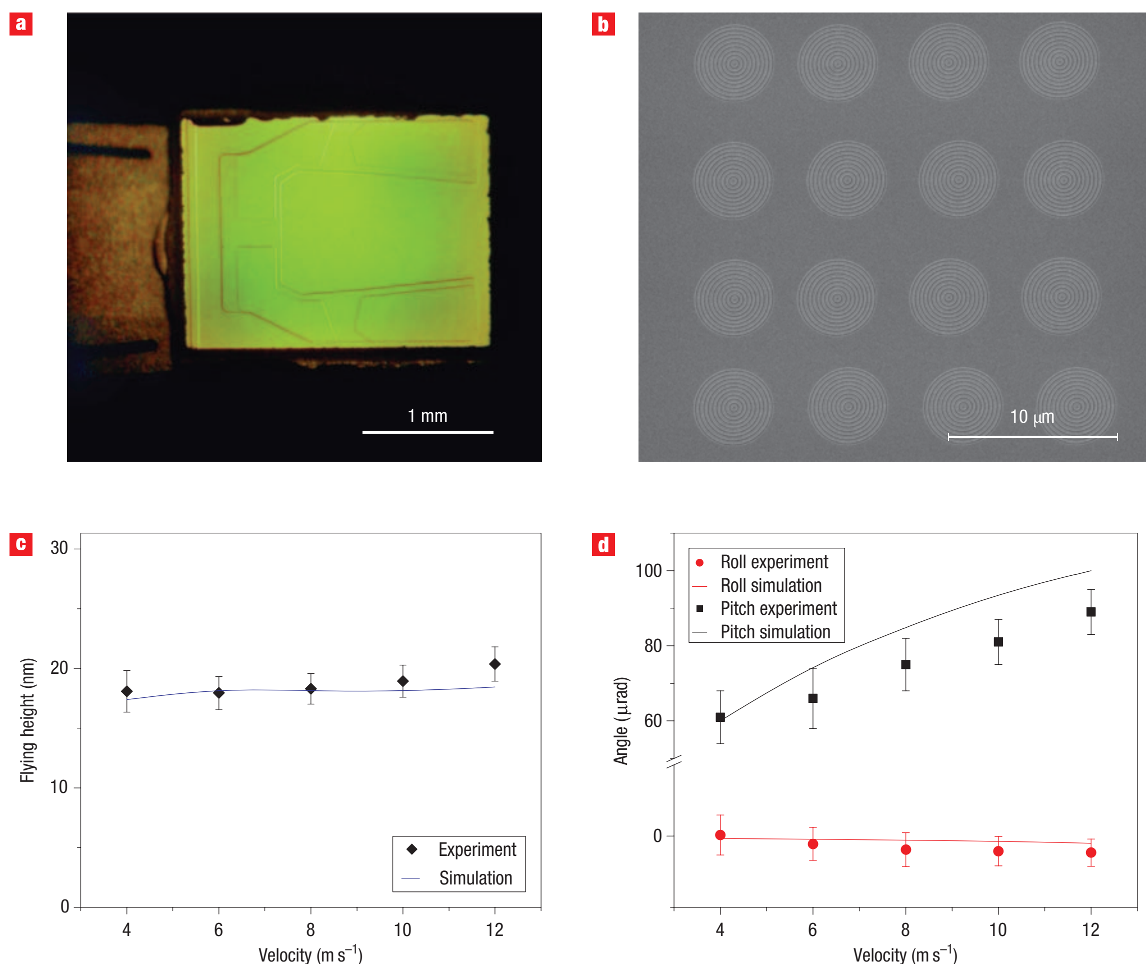

Figure 3 Fabricated plasmonic flying head and flying height measurement. a, Optical micrograph of a plasmonic flying head assembled with suspension. **b**, Scanning electron microscopy (SEM) image of an array of plasmonic lenses fabricated on an ABS. **c**, Measured and calculated flying height shows the slider maintains the flying height at 20 ± 2 nm, with scanning speeds between 4 and 12 m s^{-1}. **d**, Measured and simulated pitch and roll angle at scanning speeds between 4 and 12 m s^{-1}. Agreement between experiment and simulation demonstrates that the parallelism achieved is within the gap tolerance of 30 nm over the whole area of the plasmonic lens array and the substrate.

arrays and the rotating substrate, which is covered with photoresist. With the high bearing stiffness and small actuation mass, this self-adaptive method can provide an effective bandwidth up to 120 kHz. The use of an ABS eliminates the need for a feedback control loop and therefore overcomes the major technical barrier for high-speed scanning. It can be seen in Fig. 1 that high-throughput nanolithography is accomplished using the plasmonic flying head at a relatively high speed. The plasmonic flying head is made of a specially designed transparent air-bearing slider with arrays of plasmonic lenses fabricated on its bottom surface. Using large arrays of plasmonic lenses enables parallel writing for high throughput.

In this work, the plasmonic flying heads were fabricated using microfabrication techniques and focused ion-beam milling (see Supplementary Information), and they were evaluated using a dynamic flying height tester (DFHT IV, Phase Metrics). The plasmonic lens was numerically designed and simulated, with the result showing an intensity enhancement factor of 100× and a focused spot of 80 nm, as shown in Fig. 2a,b. Considering a focal spot within 10% variation as a criterion, numerical simulation shows that a flying height within the range 0–30 nm is acceptable (see Supplementary Information). Given this, the parallelism between the plasmonic lens array and substrate needs to be carefully considered in the design of the ABS. The ABS for the plasmonic flying head was designed using in-house developed air-bearing simulators[22]. The goal was to achieve a consistent flying height of 20 nm at scanning speeds between 4 and 12 m s^{-1}, taking into consideration the fact that disk linear velocity reduces and the skew angle changes as the head goes from the outer to inner radius. Figure 2c,d shows the ABS design and a simulated air-bearing pressure profile. The ABS design consists of a four-pad U-shaped dual-rail with a long front bar (Fig. 2c). Two large rear pads generate the repelling peak pressure to float the flying head and prevent possible physical contact (Fig. 2d). The two front pads produce the steering repelling pressure to increase bearing roll stiffness and minimize the roll angle. A sub-2 μrad roll angle is achieved across the disk by adjusting the detailed shape and depth of the rail and pads. The pitch angle is designed to be ∼80 μrad rather than even smaller to compensate for the curvature variations of both the slider and disk. By throttling injecting air from the leading edge, the long-bar design can significantly reduce the slider's pitch angle and

© 2008 Macmillan Publishers Limited. All rights reserved.

contamination sensitivities, and also enhance the slider's damping. The U-shaped dual-rail design efficiently increases the overall sub-ambient ('negative') pressure, which improves both the slider's stability and bearing stiffness. As the disk velocity decreases, both the positive pressure and negative pressure decrease, which results in lower flying height and bearing stiffness. The effective air bearing stiffness and damping ratio are about 2×10^5 N m^{-1} and 0.1, respectively. The design provides ~85 kHz effective bandwidth for gap control. The flying plasmonic lens array in the optical near field is inspired by the magnetic recording head in hard disk drives (HDD). Unlike a conventional HDD ABS[23], which uses only the trailing-edge-mounted transducer to serially read and write the magnetic bits, we designed the plasmonic head to contain a relatively large area filled by plasmonic lenses that enable parallel writing and high throughput. Owing to the rapid decay of light intensity in a plasmonic lens, all plasmonic lenses need to maintain the distance to the rotating substrate within 30 nm, which requires the bottom surface to be parallel to the substrate to within 100 μrad tilt. This stringent parallelism requirement made the design of the plasmonic head both very challenging and also different from magnetic head sliders. For example, to fly 1,000 lenses within the 30 nm gap tolerance over the usable area of 800 × 20 μm on the rear pads with each plasmonic lens of size 4 μm in diameter, the ABS has to be designed with <100 μrad pitch angle and 2 μrad roll angle. Also, the ABS needs a larger air-bearing stiffness, higher damping ratio and better contamination insensitivity than conventional ABS (see Supplementary Information). In addition, the plasmonic head must be transparent to light.

Figure 3a shows an optical microscope image of the fabricated plasmonic flying head where the sapphire ABS coated with a metal film was assembled with the suspension, and a scanning electron microscopy (SEM) image of a two-dimensional array of plasmonic lenses (4 x 4) fabricated on the ABS in a square lattice (Fig. 3b). Figure 3c,d shows the flying height and pitch and roll angle measurements, together with simulation results. We observed that the flying height is maintained over the velocity range 4–12 m s^{-1}. The measured flying height is in good agreement with the simulated ABS design performance, with slight variation from 18.0 to 20.4 nm, which is within the tolerance of 30 nm (Fig. 3c). The parallelism of the ABS is determined by the roll and pitch angles of the ABS with respect to the substrate. Under the above linear velocity range, the experimental measured roll and pitch angle varies from 0.15 to −2.34 μrad and 61 to 89 μrad, respectively, in good agreement with simulation design, which ensures the entire 1,000-lens array is within the 30 nm gap tolerance.

In the lithography experiment, a UV continuous-wave laser was focused down to a spot of several micrometres onto a plasmonic lens, which further focused the beam to a sub-100 nm spot onto the spinning disk for writing of arbitrary patterns (Fig. 1). The laser pulses were controlled by an electro-optic modulator according to the signals from a pattern generator. The writing position was referred to the angular position of the disk from the spindle encoder and the position of a piezo-stage along the radial direction. We used an inorganic TeO_x-based thermal photoresist[24] deposited on a glass disk by magnetic sputtering (see Supplementary Information). A spindle was used to rotate the disk at 2,000 r.p.m., which is equivalent to a linear speed of 10 m s^{-1} at the outer radius. After pattern writing and development in diluted KOH solution, the patterns were examined using an atomic force microscope (AFM). The result demonstrated that we can achieve high-speed patterning with 80 nm linewidths at 10 m s^{-1} (Fig. 4a). Figure 4b,c demonstrates the successful patterning of arrays of the acronym 'SINAM' with

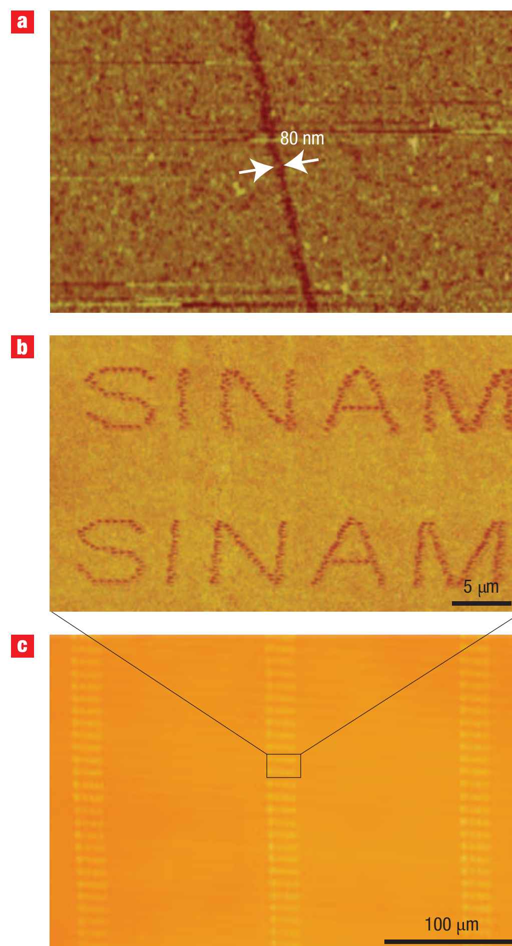

Figure 4 **Maskless lithography by flying plasmonic lenses at the near field.** **a**, AFM image of a pattern with 80 nm linewidth on the TeO_x-based thermal photoresist. **b**, AFM image of arbitrary writing of 'SINAM' with 145 nm linewidth. **c**, Optical micrograph of patterning of the large arrays of 'SINAM'.

a feature size of 145 nm. The pattern writing in the radial direction involved a coordinate transformation with Cartesian coordinates.

The resolution could be improved by careful design using shorter plasmon wavelength and guiding mechanisms, and theoretical simulation shows it could reach down to 5–10 nm (ref. 25). Owing to the fast scanning that is possible, a single plasmonic lens already has higher throughput than most other maskless lithography approaches. The throughput of plasmonic nanolithography could be greatly enhanced by using a larger number of plasmonic lenses for parallel writing. Let us consider a 1,000-lens array occupying an area of 800 × 20 μm at the bottom of the ABS, with each plasmonic lens having a diameter of 4 μm. Taking into account the changes in the mean flying height, as well as pitch and roll angles at different linear velocities, our simulation shows that the corresponding flying height variation for all the plasmonic lenses is in the range 18–24 nm, which is well within the acceptable range of 0–30 nm. Thus, at a scanning speed of 10 m s^{-1}, a plasmonic flying head carrying 1,000 lenses could write a 12 in. wafer in 2 min. Furthermore, a slider a few millimetres in size may take up to 1×10^5 lenses. Flying plasmonic lens arrays could form the

© 2008 Macmillan Publishers Limited. All rights reserved.

basis of nanofabrication techniques with throughputs that are two to five orders of magnitude higher than conventional maskless techniques.

As with any approach to maskless lithography, a number of engineering challenges—such as pattern data management, lithography linewidth control, pattern overlay and resist defect reduction—will need to be addressed before this approach can be introduced into real-world nanomanufacturing applications. Integrated approaches for precision engineering, metrology, as well as new resist development will be needed. This high-speed technique could also be used for nanoscale metrology and imaging. Such a low-cost, high-throughput scheme promises a new route towards the next generation of nanomanufacturing.

Received 31 March 2008; accepted 16 September 2008; published 12 October 2008.

References

1. Okazaki, S. Resolution limits of optical lithography. *J. Vac. Sci. Technol. B* **9**, 2829–2833 (1991).
2. Jeong, H. J. *et al*. The future of optical lithography. *Solid State Technol.* **37**, 39–47 (1994).
3. Melngailis, J. Focused ion-beam technology and applications. *J. Vac. Sci. Technol. B* **5**, 469–495 (1987).
4. Cooper, E. B. *et al*. Terabit-per-square-inch data storage with the atomic force microscope. *Appl. Phys. Lett.* **75**, 3566–3568 (1999).
5. Piner, R. D., Zhu, J., Xu, F., Hong, S. & Mirkin, C. A. 'Dip-pen' nanolithography. *Science* **283**, 661–663 (1999).
6. Vettiger, P. *et al*. The 'Millipede'—more than one thousand tips for future AFM data storage. *IBM J. Res. Develop.* **44**, 323–340 (2000).
7. Groves, T. R. & Kendall, R. A. Distributed, multiple variable shaped electron beam column for high throughput maskless lithography. *J. Vac. Sci. Technol. B* **16**, 3168–3173 (1998).
8. McCord, M. A. Electron beam lithography for 0.13 μm manufacturing. *J. Vac. Sci. Technol. B* **15**, 2125–2129 (1997).
9. Muraki, M. & Gotoh, S. New concept for high-throughput multielectron beam direct write system. *J. Vac. Sci. Technol. B* **18**, 3061–3066 (2000).
10. Pease, R. F. *et al*. Prospect of charged particle lithography as a manufacturing technology. *Microelectron. Eng.* **53**, 55–60 (2000).
11. Menon, R., Patel, A., Gil, D. & Smith, H. I. Maskless lithography. *Mater. Today* **8**, 26–33 (February 2005).
12. Salaita, K. *et al*. Massively parallel dip-pen nanolithography with 55,000-pen two-dimensional arrays. *Angew. Chem. Int. Ed.* **45**, 7220–7223 (2006).
13. Pease, R. F. Maskless lithography. *Microelectron. Eng.* **78–79**, 381–392 (2005).
14. Ritchie, R. H. Plasma losses by fast electrons in thin films. *Phys. Rev.* **106**, 874–881 (1957).
15. Barnes, W. L., Dereux, A. & Ebbesen, T. W. Surface plasmon subwavelength optics. *Nature* **424**, 824–830 (2003).
16. Genet, C. & Ebbesen, T. W. Light in tiny holes. *Nature* **445**, 39–46 (2007).
17. Fang, N., Lee, H., Sun, C. & Zhang, X. Sub-diffraction-limited optical imaging with a silver superlens. *Science* **308**, 534–537 (2005).
18. Srituravanich, W., Fang, N., Sun, C., Luo, Q. & Zhang, X. Plasmonic nanolithography. *Nano Lett.* **4**, 1085–1088 (2004).
19. Luo, X. & Ishihara, T. Surface plasmon resonant interference nanolithography technique. *Appl. Phys. Lett.* **84**, 4780–4782 (2004).
20. Liu, Z. *et al*. Focusing surface plasmons with a plasmonic lens. *Nano Lett.* **5**, 1726–1729 (2005).
21. Ozbay, E. Plasmonics: Merging photonics and electronics at nanoscale dimensions. *Science* **311**, 189–193 (2006).
22. Juang, J., Bogy, D. B. & Bhatia, C. S. Design and dynamics of flying height control slider with piezoelectric nanoactuator in hard disk drives. *ASME J. Tribol.* **129**, 161–170 (2007).
23. Han, Y., Liu, B. & Huang, X. High air-bearing stiffness slider design. *J. Magn. Magn. Mater.* **303**, 76–80 (2006).
24. Ito, E., Kawaguchi, Y., Tomiyama, M., Abe, S. & Ohno, E. TeO_X-based film for heat-mode inorganic photoresist mastering. *Jpn J. Appl. Phys.* **44**, 3574–3577 (2005).
25. Stockman, M. I. Nanofocusing of optical energy in tapered plasmonic waveguides. *Phys. Rev. Lett.* **93**, 137404 (2004).

Supplementary Information accompanies this paper at www.nature.com/naturenanotechnology.

Acknowledgements

The authors are grateful to Zhaowei Liu and Dongmin Wu for their helpful discussions. This work was financially supported by the NSF Centre for Scalable and Integrated NanoManufacturing (SINAM) (grant no. DMI-0327077) and in collaboration with Computer Mechanics Laboratory (CML) of University of California, Berkeley.

Author contributions

X.Z. conceived the idea of using a plasmonic lens to do lithography and the idea of using an air bearing to fly a plasmonic lens array at near field for high-speed lithography and imaging, and also guided the system development and experiments. C.S., W.S. and L.P. designed and developed the optical and mechanical systems. W.S. and Y.W. fabricated the plasmonic lens arrays and the flying heads. L.P. and D.B.B. designed the air-bearing and tested the flying heads. W.S., L.P., Y.W. and C.S. conducted the experiments on plasmonic lithography.

Author information

Reprints and permission information is available online at http://npg.nature.com/reprintsandpermissions/. Correspondence and requests for materials should be addressed to X.Z.

© 2008 Macmillan Publishers Limited. All rights reserved.